Validation of a strategy for cancer therapy, delivering aminoglycoside drugs to mitochondria in HeLa cells

Jiro Abe[1,2,3], Yuma Yamada[2,3], Hideyoshi Harashima[2,*]

[1]Department of Pediatrics, Graduate School of Medicine, Hokkaido University, Kita-15, Nishi 7, Kita-ku, Sapporo 060-8638, Japan

[2]Laboratory for molecular design of pharmaceutics, Faculty of Pharmaceutical Sciences, Hokkaido University, Kita-12, Nishi-6, Kita-ku, Sapporo 060-0812, Japan.

[3] These authors equally contribute this study.

*Corresponding author: Laboratory for molecular design of pharmaceutics, Faculty of Pharmaceutical Sciences, Hokkaido University, Kita-12, Nishi-6, Kita-ku, Sapporo 060-0812, Japan
Tel: +81-11-706-3919 Fax: +81-11-706-4879
E-mail: harasima@pharm.hokudai.ac.jp

Keywords: targeted drug delivery; liposomes; nanotechnology; biomaterials; cancer

Abstract

Mitochondria in human cancer cells have been implicated in cancer cell proliferation, invasion, metastasis and even drug resistance mechanisms, making them a potential target organelle for the treatment of human malignancies. Gentamicin (GM), an aminoglycoside drug, is a small molecule that functions as an antibiotic and has ototoxic and nephrotoxic characteristics. Thus, the delivery of GM to mitochondria in cancer cells would be an innovative anticancer therapeutic strategy. In this study, we attempted mitochondrial delivery of GM in HeLa cells derived from a human cervical cancer. For the mitochondrial delivery, we used MITO-Porter, a liposomal nanocarrier for mitochondrial delivery *via* membrane fusion. We first encapsulated GM in the aqueous phase of the carrier to construct GM–MITO-Porter. Flow cytometry analysis and fluorescent microscopy observations permitted us to confirm that the GM–MITO-Porter was efficiently taken up by HeLa cells and accumulated in mitochondria, while naked GM was not taken up by the cells. Moreover, cell viability assays using HeLa cells showed that the GM–MITO-Porter induced strong cytotoxic effects related to mitochondrial disorder. This finding is the first report of the mitochondrial delivery of an aminoglycoside drug to cancer cells for cancer therapeutic strategy.

1. Introduction

Waksman discovered streptomycin from Streptomyces spp. in 1944[1], and such aminoglycoside drugs (AGs) are now clinically used in treating infections caused by gram-negative bacteria with a broad antibiotic spectrum all over the world. Some AGs, for example gentamicin (GM), are preferred for use because of their low cost and higher safety by therapeutic drug monitoring, although AGs can cause irreversible hearing loss and renal toxicity caused by mitochondrial damage, the detailed mechanisms responsible for this remain unclear[2]. Mitochondria in the epidermal cells in the organ of Corti or kidneys are vulnerable to AGs[3], thus the patients with mitochondrial disease have a higher risk for AGs[4]. Actually unexpected adverse effects of AGs have been reported among patients with undiagnosed mitochondrial disease[5].

On the other hand, mitochondria in human cancer cells are closely related to cancer cell proliferation, invasion, metastasis and even drug resistance mechanisms, because of the power exerted by cancer cells for the production of usable energy [6-8]. Thus, we hypothesized that the cellular uptake of AGs could kill cancer cells *via* mitochondrial toxicity, which would lead to an effective strategy for treating cancer in a different way from conventional anticancer agents. It is well known that AGs are efficiently internalized into ear hair cells[3] and kidney distal tubule cells[9] *via* non-selective cation channels such as the Transient receptor potential vanilloid 4 (TRPV4)[10], the studies regarding cellular uptake of AGs by cancer cells have not been examined. To date, our knowledge of the anti-tumor effect of AG remains limited, probably because the internalization of AG into cancer cells without specific channels would be difficult. To overcome the first barrier to kill cancer cells *via* the mitochondrial toxicity of AG, the efficient cellular uptake of AG is required.

We previously developed MITO-Porter, a nanocarrier to deliver nucleic acids, proteins, or certain types of small molecules to mitochondria via membrane fusion [11-14]. To date, we showed that the MITO-Porter was efficiently taken up by HeLa cells derived from a human cervical cancer, and bio functional cargoes that regulate mitochondrial function were delivered to mitochondria. Here, we validated that the mitochondrial delivery of GM (a model AG) using the MITO-Porter resulted in the killing of HeLa cells *via* mitochondrial pharmacodynamics (Fig. 1). Octaarginine (R8)[15,16] modified on the surface of the MITO-Porter plays important roles in cellular uptake and mitochondrial targeting. It is expected that GM would be delivered to the mitochondrial interior, thus permitting GM to exert a pharmacological effect.

We first prepared a MITO-Porter encapsulating GM conjugated with 7-nitrobenz-2-oxa-1, 3-diazole (NBD) (a fluorescent-dye), GM-MITO-Porter and evaluated its physicochemical properties including diameters and ζ potentials. We then performed flow cytometry to assess the cellular uptake of the GM-MITO-Porter, and observed the intracellular trafficking of the carrier. We

also quantified the mitochondrial targeting rate based on obtained images. Moreover, a comparison of cell toxicity between the GM-MITO-Porter and naked NBD-GM was performed by a cell viability assay. Finally, we validated the correlation between the mitochondrial delivery of NBD-GM and cell toxicity.

2. Materials and Methods

2.1. Materials

Gentamicin Sulfate was purchased from Wako Pure Chemical Industries, Ltd (Osaka, Japan) and 4-fluoro-7-nitro-2,1,3-benzoxadiazole (NBD-F) from Tokyo Chemical Industry Co., Ltd (Tokyo, Japan). The Gentamicin Sulfate was conjugated with NBD-F to synthesize NBD-GM, which was purified as previously reported[17], and then freeze-dried (see Supplementary materials for the details). In this experiment, NBD-GM was used as a naked GM and packaged in the MITO-Porter. 1,2-Dioleoyl-sn-glycero-3-phosphatidyl ethanolamine (DOPE), egg phosphatidylcholine (EPC) were purchased from Avanti Polar lipids (Alabaster, AL). Sphingomyelin (SM) was purchased from Sigma (St. Louis, MO). Stearylated octaarginine (STR-R8) was obtained from Kurabo Industries Ltd. (Osaka, Japan). HeLa human cervix carcinoma cells were obtained from RIKEN Cell Bank (Tsukuba, Japan). Dulbecco's modified Eagle's medium (DMEM), fetal bovine serum (FBS) and MitoTracker Deep Red FM were purchased from the Invitrogen Corporation (Carlsbad, CA). All other chemicals used were commercially available reagent-grade products.

2.2. Construction of GM–MITO-Porter

We prepared GM–MITO-Porter by the reverse phase evaporation method [18]. The GM-MITO-Porter contains NBD-GM in the aqueous phase of the carrier. A suspension containing 500 µl of chloroform containing 2.75 µmol lipids [DOPE/SM = 9:2 (molar ratio)], 500 µl of diisopropyl ether and 500 µl of 10 mM HEPES buffer (pH 7.4) including 5 µmol NBD-GM, was prepared in a glass tube. The resulting suspension was sonicated *via* a small-size digital homogenizer (20KHz; Emerson Electric Co., St Louis, MO) and evaporation of the organic solvent, followed by sonication using a bath-type sonicator (85 W; Aiwa Company, Tokyo, Japan) and mixed with an STR-R8 solution (10mol% of total lipid) to prepare the GM–MITO-Porter. The lipid compositions of the GM-MITO-Porter and control liposomes (GM-R8-EPC-LP, GM-DOPE-LP) are summarized in Table 1. Unencapsulated NBD-GM was separated by ultracentrifugation (74,000*g*, 20 min, 4ºC) three times using HIMAC (Hitachi Koki Co., Ltd., Tokyo, Japan). The encapsulation efficiency of

the NBD-GM into MITO-Porter was estimated, as described in the Supplementary materials. The diameters and ζ-potentials were measured using Zetasizer Nano ZS (Malvern Instruments, Worcestershire, UK), as previously reported[22].

2.3. Evaluation of the cellular uptake of the GM–MITO-Porter by flow cytometry

Cellular uptake of the GM-MITO-Porter was quantified, as previously reported (see the reference [22] for the detailed methods). Briefly, HeLa cells (1×10^5 cells/well) were seeded on a six-well plate (Corning Inc., Corning, NY) with DMEM, containing 10% FBS, under an atmosphere of 5% CO_2 /air at 37°C for 24 h. The carriers were added to the HeLa cells (final concentration of the total lipid, 27.5 μM) for the experiment of Fig. 2. The final concentrations of NBD-GM encapsulated in carriers were used at 4, 6, 10 μM for the experiment of Fig. 4B. To validate the cellular uptake of the naked NBD-GM (Fig. 2), the cells were also treated with only NBD-GM at a high applied dose (final concentration of NBD-GM, 1000 μM). The cells were then incubated in serum-free medium for 1 h, followed by removing the medium. After the cells were washed, the cells were analyzed by flow cytometry (FACScan, Becton Dickinson, Franklin Lakes, NJ) and CellQuest software (Becton Dickinson). The cells were excited with a 488 nm light, and the fluorescence detection channel was set to a 530 nm FL1 filter. The cellular uptake is expressed as the mean fluorescence intensity (MFI).

2.4. Intracellular observation of GM–MITO-Porter using confocal laser scanning microscopy (CLSM)

The intracellular trafficking of carriers was observed using CLSM, as previously reported (see the reference[22] for the detailed methods). Briefly, HeLa cells (5×10^4 cells/well) were cultured in 3.5 cm glass-base dish (Iwaki, ASAHI GLASS Co., Ltd, Tokyo, Japan) with DMEM, which contained 10% FBS, under an atmosphere of 5% CO_2/air at 37°C for 24 h. The carriers (final concentration of total lipid, 13.75 μM) were added to the HeLa cells for the experiments of Figs. 3A, 3B. The final concentrations of NBD-GM encapsulated in GM-MITO-Porter were used at 4, 6, 10 μM for the experiment of Fig. 3C. The cells were incubated in phenol red-free medium without serum under an atmosphere of 5% CO_2/air at 37°C for 1 h, the medium was then replaced with fresh phenol red-free medium containing serum, followed by further a 100 min incubation. Before observation, mitochondria were stained with MitoTracker Deep Red FM (final concentration, 100 nM) for 10 min incubation. After washing the cells, the intracellular trafficking was observed by CLSM (FV10i- LIV; Olympus Corporation, Tokyo, Japan) equipped with a water-immersion

objective lens (UPlanSApo 60×/NA = 1.2) and a dichroic mirror (DM473/635). The cells were excited with a 473nm light for detecting NBD-GM, and a 635nm light for detecting MitoTracker Deep Red FM from a LD laser. The two fluorescence detection channels (Ch) were set to the following filters: Ch1: BP 490-540 (green color) for NBD–GM, and Ch2: BP 660-710 (red color) for MitoTracker Deep Red FM.

2.5. Calculation of mitochondrial targeting rate and mitochondrial occupation rate

We estimated mitochondrial targeting rate and mitochondrial occupation rate of the carriers using Image Pro-Plus software (ver7.0.; Ropper Industries, Sarasota, FL), as described below. Fluorescent images were captured using a FV10i- LIV microscope, as shown in Fig. 3A. The yellow pixel areas where NBD-GM (green color) co-localized with mitochondria (red color) were marked in each image. The yellow, green and red pixel areas of each cluster in the cell were separately summed for each image, and the values in each image were further summed, as previously reported (see the reference [19] for the detailed methods). S (yellow), S (green) and S (red) represent the total area of the NBD-GM that was colocalized with the mitochondria, all of the NBD-GM inside the cell and the mitochondrial region in the total cell. Mitochondrial targeting rate (Fig. 3B) was calculated as follows;

$$\text{Mitochondrial targeting rate (\%)} = S\,(\text{yellow}) / (S\,(\text{yellow}) + S\,(\text{green})) \times 100$$

This value indicates the mitochondrial targeting efficiency of the carriers, which is expected to be dependent on the intracellular trafficking of carriers to access mitochondria, not the cellular uptake process. Mitochondrial occupation rate (Fig. 3C) was calculated as follows;

$$\text{Mitochondrial occupation rate (\%)} = S\,(\text{yellow}) / S\,(\text{red}) \times 100$$

This value was used to evaluate the accumulation of the NBD-GM in mitochondria and is affected by the cellular uptake of the NBD-GM.

2.6. Evaluation of Cell Viability

The cell viability was evaluated using WST-1 reagent (Takara BIO Inc., Shiga, Japan), as previously reported (see the reference[22] for the detailed methods). Briefly, HeLa cells (1×10^4 cells/well) were incubated in a 24 well plate (Greiner Bio-One GmbH, Frickenhausen, Germany)

with DMEM containing 10% FBS, under an atmosphere of 5% CO_2 /air at 37°C for 24 h. The cells were incubated with sample suspensions in 250 μl of serum-free DMEM under an atmosphere of 5% CO_2 /air at 37°C for 2 h, and the medium was then replaced with DMEM containing serum, followed by incubation for a further 48 h.

The cell viability was measured using a WST-1 Reagent by an EnSpire™ 2300 Multilabel Reader (PerkinElmer, Waltham, MA). The value of cell viability was calculated as follows;

Cell viability (%) = $V_S/V_U \times 100$,

where V_S and V_U represent the cell viability for treated and untreated cells with samples, respectively.

2.7. Statistical analysis

The cellular uptake of NBD-GM by the carriers were evaluated in Fig. 2B, and the statistical significance between the non treatment and others were calculated by one-way ANOVA, followed by the Bonferroni/Dunn test. In Fig. 3B, the mitochondrial targeting rates were evaluated and the statistical significance between the GM-MITO-Porter and GM-R8-EPC-LP were calculated by the student t-test. In Fig. 4A, cellular viabilities were evaluated, and statistical significances were calculated between naked NBD-GM and others by one-way ANOVA, followed by the Bonferroni/Dunn test. In Fig. 4B, the cellular uptake was evaluated and statistical significances between the GM-MITO-Porter and GM-R8-EPC-LP were calculated by the student t-test. Levels of p values < 0.05 were considered to be significant.

3. Results

3.1. Construction of the GM-MITO-Porter

We used NBD-GM for the encapsulation in the MITO-Porter, where the mitochondria-fusogenic lipid composition was used[11,12]. After the synthesis and purification of the NBD-GM, we performed a competitive enzyme immunoassay to evaluate the antibacterial activity of NBD-GM using a MaxSignal Gentamicin ELISA Test Kit (Bio Scientific Corporation, Austin, TX). The findings showed that the activity of the NBD-GM was 52 ± 19% of the antibacterial activity of the unconjugated GM (n=3).

Using a reverse phase evaporation method, we succeeded in preparing a GM-MITO-Porter in which the nanoparticles were positively charged (147 ± 6 nm, 44 ± 4 mV, n=3)

and the encapsulation efficiency of the GM in the MITO-Porter was 6 ± 2% (n=3). Although the encapsulation efficiency appeared to be low, it was within the value expected for encapsulating very hydrophilic and cationic low-weight molecules[20]. We checked the stability of the GM-MITO-Porter, and confirmed that the diameter and ζ-potential were stable in the liquid at 4°C for one month (Fig. S1). The GM-MITO-Porter was equipped with STR-R8 as a cellular uptake device [15,16]. In this experiment, we also prepared a GM-R8-EPC-LP with high cellular uptake and low mitochondrial fusion activities and a GM-DOPE-LP with low cellular uptake and mitochondrial fusion activities. The diameters of the prepared carriers were comparable (approximately 100-200 nm) as shown in Table 1. The ζ-potentials of the GM-MITO-Porter and the R8-EPC-LP were positively charged, suggesting that the cationic R8 was displayed on the carrier surface.

3.2. Evaluation of cellular uptake of GM-MITO-Porter

Although it is well known that GM is efficiently internalized into ear hair cells and kidney distal tubule cells[3,9], it has not been demonstrated that GM can be taken up by cancer cells. Therefore, we first evaluated the cellular uptake of NBD-GM as naked GM using HeLa cells as model cancer cells by flow cytometry (Fig. 2). The fluorescence intensities of the NBD-GM taken up by the cells were comparable to that of non-treated cells, indicating a low cellular uptake of naked NBD-GM in the case of HeLa cells. Intracellular observations also showed that NBD-GM was not taken up by the HeLa cells (Fig. S2A). On the other hand, in the case of Pheochromocytoma cell 12 (PC12) cells where TRPV4 was found to be highly expressed[21], the NBD-GM was efficiently internalized into the cells (Fig. S2B). We also performed an RT-PCR assay to detect TRPV4-mRNA, resulting in the observation of the gene expression of TRPV4 in the case of PC12 cells, while this was not observed in the case of HeLa cells (Fig. S3). These results indicate that the first barrier for killing cancer cells *via* mitochondrial toxicity by mitochondrial delivery of GM is the plasma membrane.

We previously reported that the MITO-Porter, modified with STR-R8, was efficiently internalized into HeLa cells[22,23]. Based on these reports, we hypothesized that MITO-Porter would likely permit GM to be efficiently internalized into HeLa cells. As shown in Fig. 2A, the fluorescence intensities of the NBD-GM taken up by the cells were relatively high in the case of GM-MITO-Porter and GM-R8-EPC-LP, although the value for the GM-DOPE-LP that was not modified with STR-R8 was comparable to that of naked NBD-GM. As shown in Fig. 2B, both the cellular uptakes of GM-MITO-Porter and GM-R8-EPC-LP were significantly higher than that for GM-DOPE-LP and naked NBD-GM. These results indicate that the R8 modified carriers are able to

internalize NBD-GM into HeLa cells. We used the GM-MITO-Porter and GM-R8-EPC-LP in subsequent experiments.

3.3. Intracellular observation of GM-MITO-Porter using CLSM

The final process for mitochondrial delivery includes the introduction of the cargos into the mitochondrial compartment. We observed the intracellular trafficking of the GM-MITO-Porter, GM-R8-EPC-LP and NBD-GM in HeLa cells after staining the mitochondria red (Fig. 3A). When the GM-MITO-Porter was added to HeLa cells, several yellow clusters were observed, indicating that the green labeled GM (NBD-GM) co-localized with the red stained mitochondria. Only little yellow clusters were observed in the case of GM-R8-EPC-LP, which has a low mitochondrial fusion activity.

We quantified the mitochondrial targeting rate based on the obtained images, showing that the value for the GM-MITO-Porter (12±3% (n=32)) was significantly higher than that of GM-R8-EPC-LP (4±1% (n=32)) (Fig. 3B). Moreover, we calculated the mitochondrial occupation rate (Fig. 3C), and confirmed that, in mitochondria that contained the GM-MITO-Porter, its content increased with increasing applied dose. At an applied dose of 10 μM NBD-GM, the mitochondrial occupation rate of GM-MITO-Porter was about 2.5%, while the value for GM-R8-EPC-LP was about 1/50 that of the GM-MITO-Porter (0.05 ± 0% (n=30)).

3.4. Evaluation of cellular toxicity after mitochondrial delivery of NBD-GM using the MITO-Porter system

Cellular toxicity was evaluated by means of a cell viability assay of HeLa cells after the mitochondrial delivery of NBD-GM by MITO-Porter system. The results showed that cell viability was decreased with increasing applied dose of the GM-MITO-Porter, and the effective concentration 50 (EC_{50}) was 2.2 μM of NBD-GM (circles in Fig. 4A). Meanwhile, cell viability was not decreased in the case of GM-R8-EPC-LP (squares) or NBD-GM (diamonds) (Fig. 4A), although the cellular uptake of the GM-R8-EPC-LP were comparable with the GM-MITO-Porter at same applied doses (Fig. 4B). We also observed no cell toxicity, when the empty MITO-Porter was used (Fig. S4). We also validated the relationship between cellular toxicity and the mitochondrial accumulation of NBD-GM as shown in Fig. 4C. The results showed that the toxicity steadily increased with the amount of NBD-GM in mitochondria (Fig. 4C).

4. Discussion

In previous study, it has been reported that AGs have a high affinity for ribosomal RNA and permeability transition in mitochondria, resulting in apoptosis *via* the inhibition of mitochondrial transcription or exaggerated oxidative stress, which are consistent with the molecular mechanisms for the ototoxicity and nephrotoxicity induced by AGs[24-26]. AGs have been clinically available as antibiotics for many years, and, unfortunately, can exert some irreversible adverse-effects, especially in the patients with a mitochondrial disease. AGs are not only antibiotics, but also function as latent mitochondrial toxic agents. In this study, we validated whether AGs would have anticancer activity once they are delivered into mitochondria.

However, this validation would be difficult using naked AGs because they cannot readily penetrate the cellular membrane without selective channels such as TRPV4[9,21]. As shown in Fig. 3A, NBD-GM as a model AG was not internalized into HeLa cells, which do not express high levels of TRPV4. Thus, we designed the GM-MITO-Porter, in which NBD-GM was encapsulated by mitochondrial fusogenic envelopes modified with STR-R8, i.e., a cellular uptake device. We could confirm that the GM-MITO-Porter achieved mitochondrial delivery of NBD-GM in cancer HeLa cells (Figs. 2, 3).

The mitochondrial delivery of NBD-GM using the MITO-Porter system resulted in a decreased cell viability and the effect was dose-dependent (Fig.4A), and the more the mitochondrial accumulation of NBD-GM increased, the lower was the cellular viability (Fig.4C). Irrespective of the low encapsulation efficiency, the GM-MITO-Porter had significant cellular toxicity; the EC_{50} was 2.2 μM of NBD-GM where the total lipid concentration was theoretically only about 6 μM. Based on this value, the GM-MITO-Porter would be predicted to have a therapeutic effect in the human body as a liposomal drug. Under an ideal scenario, only about 30 μmol of the total amount of lipid would be needed for each drip-in-vein to reach the EC_{50} of the blood GM concentration, assuming that the total circulating blood volume is 5 L. On the other hand, Doxil, which is a clinically available liposomal drug encapsulating doxorubicin, requires about 1 mmol of the total lipid amount for each drip-in-vein[27]. The GM-MITO-Porter might have some drug advantages, in that a smaller amount of total lipids is needed for each drip-in-vein.

It was reported that the mitochondrial toxicity of GM in ear hair cells could be induced by the inhibition of mitochondrial transcription by binding to ribosomal RNA[24] or by opening permeability transition pores by induced oxidative stress and metabolic change[25]. Thus, we hypothesized that the delivery of NBD-GM into mitochondria of cancer HeLa cells might lead to cell death *via* a mechanism similar to that reported for ear hair cells. Attention should be paid to the

typical adverse effects of GM, i.e., ototoxicity and renal toxicity, in the case of the clinical use of the GM-MITO-Porter. In this study, we simply validated whether the GM-MITO-Porter had the ability to kill cancer cells in *in vitro* experiments. Considering the administration of GM-MITO-Porter into body *via* systemic injection, it is expected that conventional liposomes such as GM-MITO-Porter would not reach inner hairy cells across the blood-labyrinthine barrier, which naked GM molecules could cross in some way[9]. Moreover, conventional liposomes with sizes of more than 100 nm access renal tubular epidermal cells with great difficulty, because the carrier needs to pass through the small pores in blood endothelial cells[28]. It is probable that the GM-MITO-Porter might prevent hearing loss and renal injury of a GM molecule, like liposomal amphotericin B, a clinically available AmBisome[29]. We plan to investigate the toxicity of the GM-MITO-Porter in *in vivo* experiments in the near future.

There have been many reports regarding multidrug resistant cancer cells and the complex mechanisms associated with this effect[30], e.g. P-glycoproteins as efflux pumps of anticancer drugs[31], which suggests that there are some limitations concerning clinically untreatable cancers by using conventional chemotherapy. The use of a MITO-Porter system for delivering agents that are toxic to mitochondria, such as GMs, may be an alternative anticancer therapeutic strategy. It is possible that the chronic administration of the GM-MITO-Porter might induce emerging bacteria that are resistant to antimicrobial therapies resulting from the transformation of *in vivo* microbiota. However it is likely that the liposomal GM would be less likely to induce emerging bacteria resistant to antibiotics than naked clinically available GM due to the fact that the GM is encapsulated by lipid bilayers and has a narrower drug biodistribution, which would efficiently isolate GM away from *in vivo* microbiota, such as human flora in the skin, digestive, or respiratory tracts.

To use the GM-MITO-Porter as a clinical application for cancer therapy, the selective targeting to cancer cells in body is required. Thus, we plan to equip the GM-MITO-Porter with *in vivo* cancer targeting ability, including the surface modification of carriers with poly ethylene-glycol to enhance tumor accumulation *via* the enhanced permeability retention effect[32-34] and ligand modification, e.g. the use of the RGD peptide[35] for integrin $\alpha_v\beta_3$, HER2 antagonistic peptide modified liposome[36] for a HER2 receptor, which some tumors specifically overexpress[37]. These studies are currently under way.

5. Conclusion

In order to investigate the intracellular dynamics and cellular toxicity of AGs using cancer HeLa cells, we constructed a GM-MITO-Porter, where NBD-GM (a model AG) with low

cellular internalization, was encapsulated into the MITO-Porter. Flow cytometry analysis and fluorescent microscopy observations permitted us to confirm that the GM–MITO-Porter achieved mitochondrial delivery of NBD-GM in cancer HeLa cells. Moreover, we showed that GM–MITO-Porter induced a strong cytotoxicity, suggesting that NBD-GM has toxicity related to mitochondrial disorder. The findings indicate that the GM-MITO-Porter has the potency of an anticancer drug *via* its mitochondrial toxicity.

Acknowledgments

This work was supported, in part by, a Grant-in-Aid for Scientific Research (B) [Grant No. 26282131 (to Y.Y.)] from the Ministry of Education, Culture, Sports, Science and Technology, the Japanese Government (MEXT), and Kobayashi Foundation for Cancer Research (to Y.Y.). We also thank Dr. Milton Feather for his helpful advice in writing the manuscript.

References

1. Comroe JH, Jr. 1978. Pay dirt: the story of streptomycin. Part I. From Waksman to Waksman. The American review of respiratory disease 117(4):773-781.

2. Kalghatgi S, Spina CS, Costello JC, Liesa M, Morones-Ramirez JR, Slomovic S, Molina A, Shirihai OS, Collins JJ 2013. Bactericidal antibiotics induce mitochondrial dysfunction and oxidative damage in Mammalian cells. Science translational medicine 5(192):192ra185.

3. Ward DT, Maldonado-Perez D, Hollins L, Riccardi D 2005. Aminoglycosides induce acute cell signaling and chronic cell death in renal cells that express the calcium-sensing receptor. Journal of the American Society of Nephrology : JASN 16(5):1236-1244.

4. Qian Y, Guan MX 2009. Interaction of aminoglycosides with human mitochondrial 12S rRNA carrying the deafness-associated mutation. Antimicrobial agents and chemotherapy 53(11):4612-4618.

5. Skou AS, Tranebjaerg L, Jensen T, Hasle H 2014. Mitochondrial 12S ribosomal RNA A1555G mutation associated with cardiomyopathy and hearing loss following high-dose chemotherapy and repeated aminoglycoside exposure. The Journal of pediatrics 164(2):413-415.

6. Ishikawa K, Takenaga K, Akimoto M, Koshikawa N, Yamaguchi A, Imanishi H, Nakada K, Honma Y, Hayashi J 2008. ROS-generating mitochondrial DNA mutations can regulate tumor cell metastasis. Science 320(5876):661-664.

7. Ashkenazi A 2015. Targeting the extrinsic apoptotic pathway in cancer: lessons learned and future directions. The Journal of clinical investigation 125(2):487-489.

8. Chamberlain GR, Tulumello DV, Kelley SO 2013. Targeted delivery of doxorubicin to mitochondria. ACS Chem Biol 8(7):1389-1395.

9. Wang Q, Steyger PS 2009. Trafficking of systemic fluorescent gentamicin into the cochlea and hair cells. J Assoc Res Otolaryngol 10(2):205-219.

10. Lee JH, Park C, Kim SJ, Kim HJ, Oh GS, Shen A, So HS, Park R 2013. Different uptake of gentamicin through TRPV1 and TRPV4 channels determines cochlear hair cell vulnerability. Exp Mol Med 45:e12.

11. Yamada Y, Akita H, Kamiya H, Kogure K, Yamamoto T, Shinohara Y, Yamashita K, Kobayashi H, Kikuchi H, Harashima H 2008. MITO-Porter: A liposome-based carrier system for delivery of macromolecules into mitochondria via membrane fusion. Biochimica et biophysica acta 1778(2):423-432.

12. Yamada Y, Harashima H 2008. Mitochondrial drug delivery systems for macromolecule and their therapeutic application to mitochondrial diseases. Adv Drug Deliv Rev 60(13-14):1439-1462.

13. Furukawa R, Yamada Y, Kawamura E, Harashima H 2015. Mitochondrial delivery of antisense RNA by MITO-Porter results in mitochondrial RNA knockdown, and has a functional impact on mitochondria. Biomaterials 57:107-115.

14. Yamada Y, Harashima H 2015. Targeting the Mitochondrial Genome via a Dual Function

MITO-Porter: Evaluation of mtDNA Levels and Mitochondrial Function. Methods in molecular biology 1265:123-133.

15. Futaki S, Suzuki T, Ohashi W, Yagami T, Tanaka S, Ueda K, Sugiura Y 2001. Arginine-rich peptides. An abundant source of membrane-permeable peptides having potential as carriers for intracellular protein delivery. J Biol Chem 276(8):5836-5840.

16. Nakase I, Niwa M, Takeuchi T, Sonomura K, Kawabata N, Koike Y, Takehashi M, Tanaka S, Ueda K, Simpson JC, Jones AT, Sugiura Y, Futaki S 2004. Cellular uptake of arginine-rich peptides: roles for macropinocytosis and actin rearrangement. Mol Ther 10(6):1011-1022.

17. Isoherranen N, Soback S 2000. Determination of gentamicins C(1), C(1a), and C(2) in plasma and urine by HPLC. Clin Chem 46(6 Pt 1):837-842.

18. Szoka F, Jr., Papahadjopoulos D 1978. Procedure for preparation of liposomes with large internal aqueous space and high capture by reverse-phase evaporation. Proc Natl Acad Sci U S A 75(9):4194-4198.

19. Kawamura E, Yamada Y, Yasuzaki Y, Hyodo M, Harashima H 2013. Intracellular observation of nanocarriers modified with a mitochondrial targeting signal peptide. Journal of bioscience and bioengineering 116(5):634-637.

20. Morgan JR, Williams KE 1980. Preparation and properties of liposome-associated gentamicin. Antimicrobial agents and chemotherapy 17(4):544-548.

21. Jang Y, Jung J, Kim H, Oh J, Jeon JH, Jung S, Kim KT, Cho H, Yang DJ, Kim SM, Kim IB, Song MR, Oh U 2012. Axonal neuropathy-associated TRPV4 regulates neurotrophic factor-derived axonal growth. J Biol Chem 287(8):6014-6024.

22. Yamada Y, Kawamura E, Harashima H 2012. Mitochondrial-targeted DNA delivery using a DF-MITO-Porter, an innovative nano carrier with cytoplasmic and mitochondrial fusogenic envelopes. J Nanopart Res 14(8):1013-1027.

23. Yamada Y, Nakamura K, Furukawa R, Kawamura E, Moriwaki T, Matsumoto K, Okuda K, Shindo M, Harashima H 2013. Mitochondrial delivery of bongkrekic acid using a MITO-porter prevents the induction of apoptosis in human hela cells. J Pharm Sci-Us 102(3):1008-1015.

24. Hobbie SN, Bruell CM, Akshay S, Kalapala SK, Shcherbakov D, Bottger EC 2008. Mitochondrial deafness alleles confer misreading of the genetic code. Proc Natl Acad Sci U S A 105(9):3244-3249.

25. Jensen-Smith HC, Hallworth R, Nichols MG 2012. Gentamicin rapidly inhibits mitochondrial metabolism in high-frequency cochlear outer hair cells. PloS one 7(6):e38471.

26. Alharazneh A, Luk L, Huth M, Monfared A, Steyger PS, Cheng AG, Ricci AJ 2011. Functional hair cell mechanotransducer channels are required for aminoglycoside ototoxicity. PloS one 6(7):e22347.

27. Fujisaka Y, Horiike A, Shimizu T, Yamamoto N, Yamada Y, Tamura T 2006. Phase 1 clinical

study of pegylated liposomal doxorubicin (JNS002) in Japanese patients with solid tumors. Jpn J Clin Oncol 36(12):768-774.

28. Dolman ME, Harmsen S, Storm G, Hennink WE, Kok RJ 2010. Drug targeting to the kidney: Advances in the active targeting of therapeutics to proximal tubular cells. Adv Drug Deliv Rev 62(14):1344-1357.

29. Walsh TJ, Goodman JL, Pappas P, Bekersky I, Buell DN, Roden M, Barrett J, Anaissie EJ 2001. Safety, tolerance, and pharmacokinetics of high-dose liposomal amphotericin B (AmBisome) in patients infected with Aspergillus species and other filamentous fungi: maximum tolerated dose study. Antimicrobial agents and chemotherapy 45(12):3487-3496.

30. Baguley BC 2010. Multiple drug resistance mechanisms in cancer. Molecular biotechnology 46(3):308-316.

31. Abdallah HM, Al-Abd AM, El-Dine RS, El-Halawany AM 2015. P-glycoprotein inhibitors of natural origin as potential tumor chemo-sensitizers: A review. Journal of advanced research 6(1):45-62.

32. Matsumura Y, Maeda H 1986. A new concept for macromolecular therapeutics in cancer chemotherapy: mechanism of tumoritropic accumulation of proteins and the antitumor agent smancs. Cancer Res 46(12 Pt 1):6387-6392.

33. Maeda H, Sawa T, Konno T 2001. Mechanism of tumor-targeted delivery of macromolecular drugs, including the EPR effect in solid tumor and clinical overview of the prototype polymeric drug SMANCS. J Control Release 74(1-3):47-61.

34. Hatakeyama H, Akita H, Harashima H 2013. The polyethyleneglycol dilemma: advantage and disadvantage of PEGylation of liposomes for systemic genes and nucleic acids delivery to tumors. Biol Pharm Bull 36(6):892-899.

35. Zhen Z, Tang W, Chen H, Lin X, Todd T, Wang G, Cowger T, Chen X, Xie J 2013. RGD-modified apoferritin nanoparticles for efficient drug delivery to tumors. ACS nano 7(6):4830-4837.

36. Stefanick JF, Ashley JD, Bilgicer B 2013. Enhanced cellular uptake of peptide-targeted nanoparticles through increased peptide hydrophilicity and optimized ethylene glycol peptide-linker length. ACS nano 7(9):8115-8127.

37. Fernandes E, Ferreira JA, Andreia P, Luis L, Barroso S, Sarmento B, Santos LL 2015. New trends in guided nanotherapies for digestive cancers: A systematic review. J Control Release 209:288-307.

Table 1 Characteristics of the carriers used in this study.

Carrier-type	Lipid composition (mol ratio)	Diameter (nm)	PDI	ζ-potential (mV)	Property
GM-MITO-Porter	DOPE/SM/STR-R8=9/2/1	147±6	0.16±0.03	44±4	***High*** mitochondrial fusogenic envelopes with cellular uptake device (R8)
GM-R8-EPC-LP	EPC/SM/STR-R8=9/2/1	119±17	0.25±0.09	32±5	***Low*** mitochondrial fusogenic envelopes with cellular uptake device (R8)
GM-DOPE-LP	DOPE/SM=9/2	205±5	0.30±0	1±2	***Low*** mitochondrial fusogenic envelopes

All types of carriers contained NBD-GM. Data denote the mean ± S.D.(n=6).

Fig. 1

Schematic image of the mitochondrial delivery of NBD-GM by the MITO-Porter system, leading to mitochondrial toxicity.

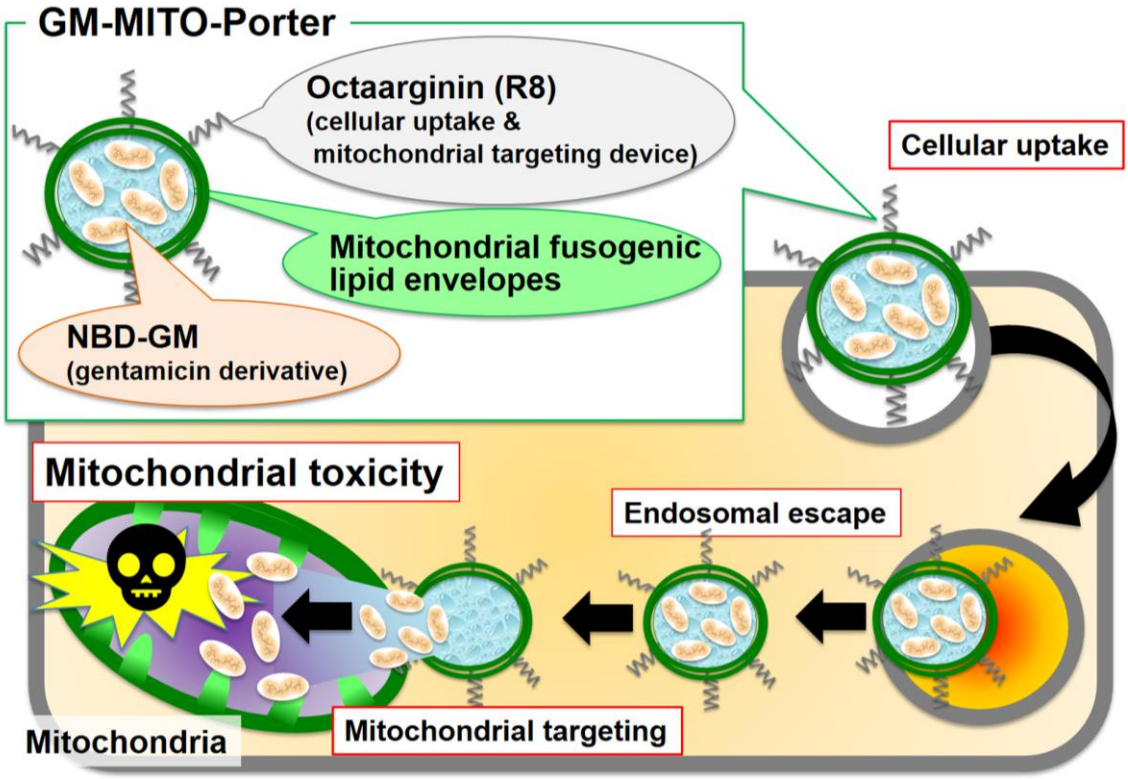

Fig. 2

Flow cytometry analysis to evaluate the cellular uptake of the GM-MITO-Porter. The histogram plot (Fig. 2A) shows the fluorescence intensities of NBD-GM taken up by HeLa cells after treatment with the GM-MITO-Porter (a), GM-R8-EPC-LP (b) and GM-DOPE-LP (c). The cells were also treated with only naked NBD-GM (d) at a high applied dose. In Fig. 2B, the cellular uptakes are expressed as the MFI. Data are represented as the mean ± SD (n=3). ** Significant differences between non treatment and others ($p<0.01$).

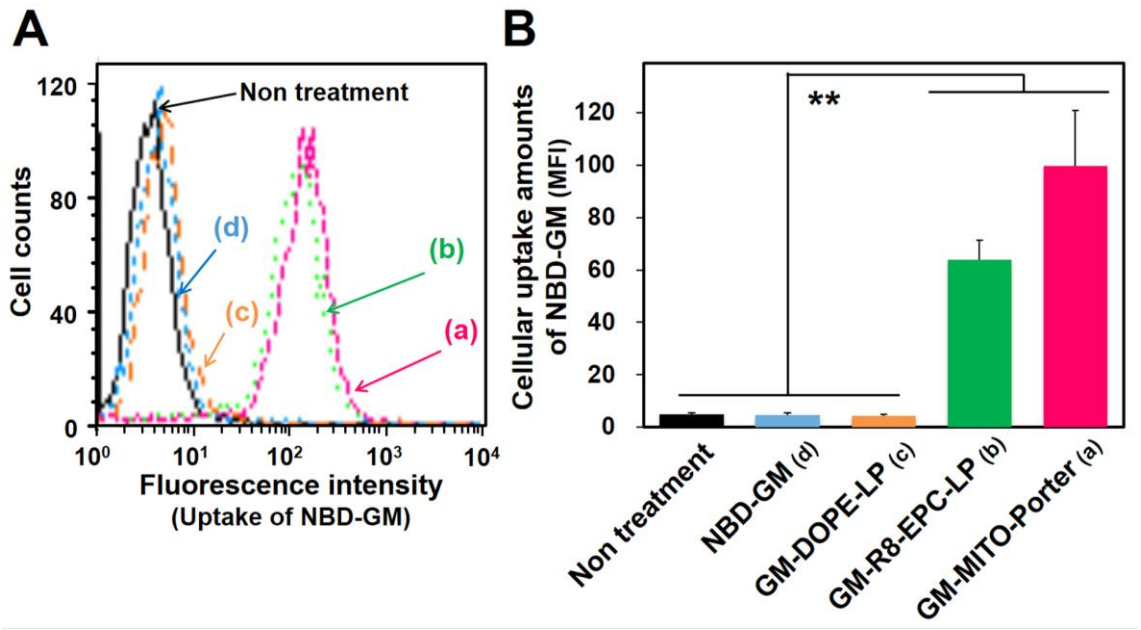

Fig. 3

Intracellular trafficking analysis of the GM-MITO-Porter. Intracellular observation of NBD-GM (green color) encapsulated in GM-MITO-Porter (upper panels) and GM-R8-EPC-LP (lower panels) using CLSM (**A**). NBD-GM is seen to co-localize with red stained mitochondria in HeLa cells, observed as yellow signals in the merged images. Scale bars, 20μm. The mitochondrial targeting rate was calculated based on the obtained images (**B**). Data are represented by the mean ± S.E.M. (n = 32-35). ** Significant differences ($p<0.01$). Mitochondrial occupation rate of GM-MITO-Porter at various applied doses of NBD-GM (**C**). Data are represented by the mean ± S.E.M. (n = 30). The value of GM-R8-EPC-LP was 0.05 ± 0% at the final concentration of 10 μM NBD–GM (n=30).

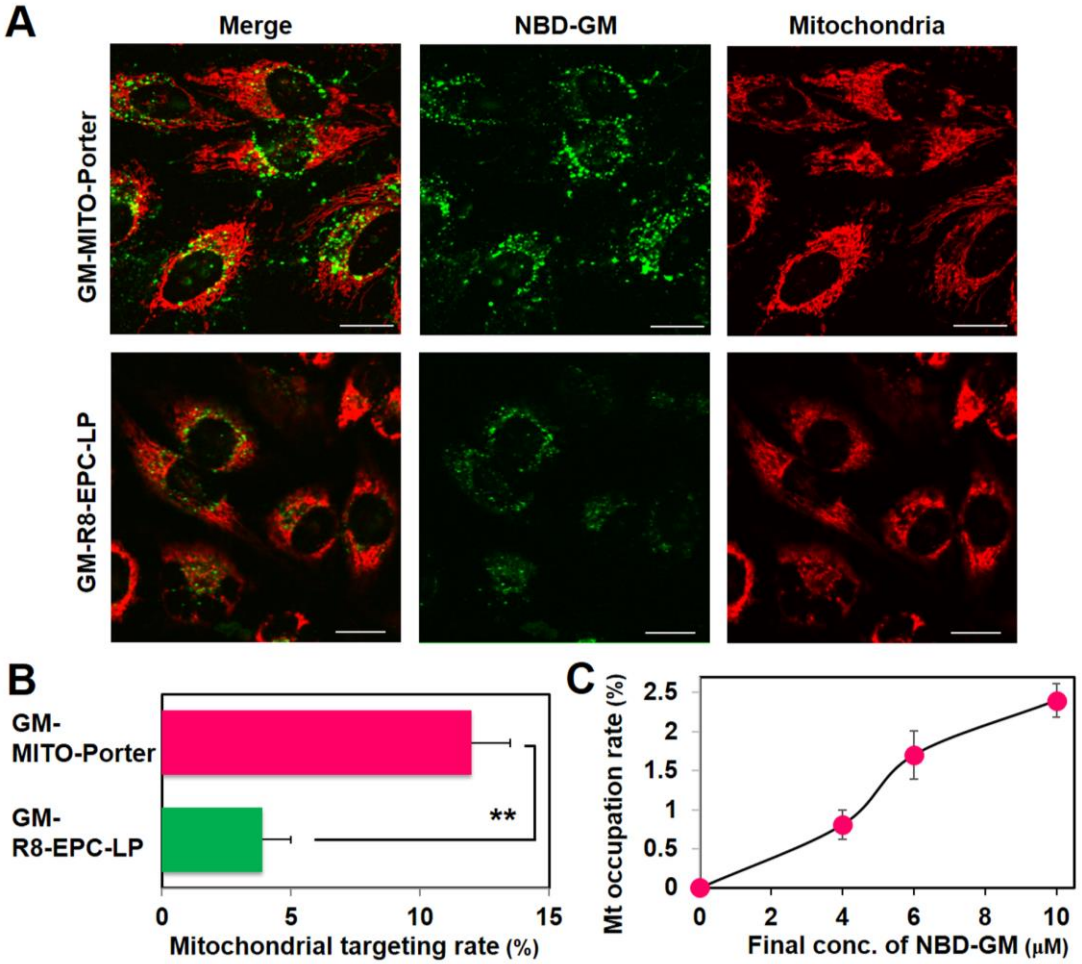

Fig. 4

Evaluation of the cellular toxicity of the GM-MITO-Porter in HeLa cells and investigation of the relationship between the toxicity and mitochondrial accumulation of NBD-GM. Comparison of cellular toxicity among the GM-MITO-Porter, R8-GM-EPC-LP and naked NBD-GM at various applied doses (**A**). The circles, squares and diamonds represent the values corresponding to cell viability (%) of the GM-MITO-Porter, R8-GM-EPC-LP and naked NBD-GM. Data are represented by the mean ± S.D. (n = 6). ** Significant differences between naked NBD-GM and the others in each concentration ($p<0.01$). Comparison of cellular uptake of GM-MITO-Porter and R8-GM-EPC-LP at various applied dose (**B**). Data are represented by the mean ± S.D. (n = 3). There are no significant differences at each concentration. Relationship between mitochondrial occupation rate and cell viability (**C**). For the x-axis (mitochondrial occupation rate), we used data shown in Fig. 3C. For the y-axis (cell viability), we used data shown in Fig. 4A.

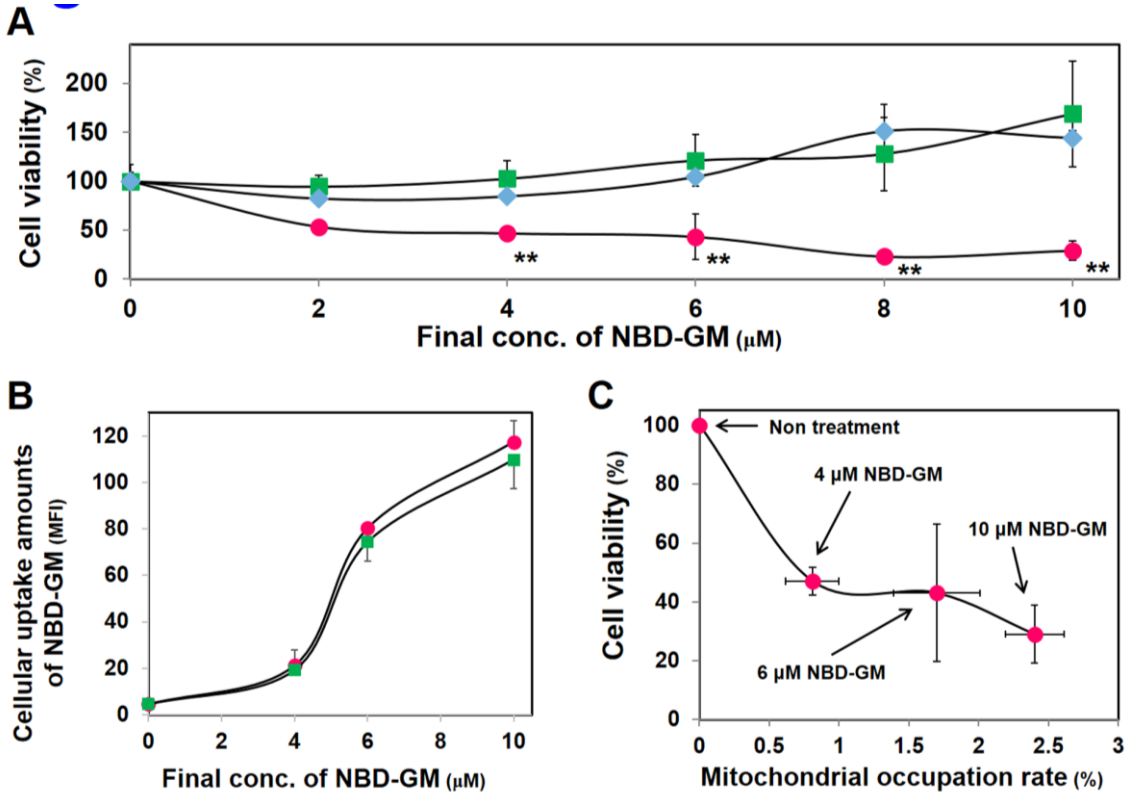

Supplementary data

Supplementary Methods

1. Synthesis and purification of NBD-GM.

The Gentamicin Sulfate was conjugated with NBD-F, which labels primary and secondary amines, to synthesis NBD-GM by chemical bonding between the amino groups of Gentamicin Sulfate and NBD-F as previously reported [1]. The synthesis was performed in a 1.5 ml tube by mixing 10 μl of 100 mM Gentamicin Sulfate water-solution (5 eq.), 2 μl of 100 mM NBD-F ethanol-solution (1 eq.) and 18 μl of 100 mM boric buffer (pH=9.0). After stirring the reaction mixture at 60°C for 10 min in the dark, the mixture was neutralized by adding 470 μl of a 5 mM HCl solution 4°C to stop the reaction. The crude NBD-GM was was purified by reversed-phase high performance liquid chromatography (reversed-phase HPLC), using an InertSustain C18 (5 μm) column (4.6 x 250 mm, GL Sciences, Tokyo, Japan) with a 30% acetonitrile water-solution. The HPLC profile was detected at 336 nm. A new peak eluted at 2 - 2.5 min, and this peak was collected as the NBD-GM, and was then freeze dried.

2. Estimation of encapsulation efficiency of the NBD-GM into MITO-Porter.

To estimate the encapsulation efficiency of the NBD-GM, a GM-MITO-Porter

containing a lipid film labeled with rhodamine-DOPE (Avanti Polar lipids, Alabaster, AL) was prepared (1 mol% rhodamine-DOPE of total lipids). The GM-MITO-Porter was separated from the unencapsulated NBD-GM by ultracentrifugation (74,000*g*, 20 min, 4^{o}C) three times using HIMAC (Hitachi Koki Co., Ltd., Tokyo, Japan) and the recovered NBD-GM and the recovered lipids were then determined after treatment with SDS (final concentration, 1%). The applied NBD-GM and the applied lipids were also determined before ultrafiltration. The amounts of NBD-GM and the amounts of lipid were determined by measuring the fluorescent intensities of the NBD-GM (excitation at 460 nm and emission at 534 nm) and the rhodamine-DOPE (excitation at 560 nm and emission at 590 nm), respectively. The encapsulation efficiency was calculated using equation shown below:

encapsulation efficiency (%) = (recovered NBD-GM / recovered lipid)/ (applied NBD-GM / applied lipid) x 100.

3. Analysis of TRPV-4 gene expression

Total RNA extraction from confluent HeLa cells, PC-12 cells or HaCaT cells (human skin keratinocyte)[2] was performed with the TRIzol Reagent (Invitrogen, Carlsbad, CA) and purification was carried out according to the conventional ethanol

precipitation followed by DNase-I treatment to digest any DNA contamination in the sample. The concentration of the obtained RNA was measured using a supersensitive NanoDrop Lite spectrophotometer (ThermoScientific, Waltham, MA). Reverse transcription was performed using the High Capacity RNA-to-cDNA Kit (Applied Biosystems, Foster City, CA). In brief, cDNA was generated from 1 μg of RNA by means of an RT Enzyme Mix according to the manufacturer's instructions on a PCR thermal cycler (C1000 Touch Thermal Cycler, Bio-Rad, Berkeley, CA). The resulting cDNA was diluted to a final concentration of 10 ng/μl for PCR amplification. Customized oligonucleotide PCR primers (Sigma Genosys Japan, Ishikari, Japan) to detect TRPV-4 and GAPDH (internal control), and cDNA templates were mixed with DNA polymerase (AmpliTaqGold 360 Master Mix, Applied Biosystems) according to the manufacture instructions in PCR amplification, carried out by using a PCR thermal cycler. The following primers were used for a human HeLa cell line and human HaCaT cell line: Homo sapience TRPV4 (Forward 5'-AGATGTACGACCTGCTGCTG-3', Reverse 5'-TCCCGCAGCAGTTCATTGAT-3), Homo sapience GAPDH (Forward 5'-CCTCTGACTTCAACAGCGAC-3', Reverse 5'-CGTTGTCATACCAGGAAATGAG-3'). The following primers were used for rat PC-12 cell line: Rattus norvegicus TRPV4 (Forward

5'-ACCACGGTGGACTACCTGAG-3, Reverse 5'-GATTCAGGAGGGTGACCAGA-3'), Rattus norvegicus GAPDH (Forward 5'-GGCAAGTTCAACGGCACAGT-3', Reverse 5'-ATGGGTTTCCCGTTGATGAC-3'). Each 4 μL of PCR products were used for electrophoresis in polyacrylamide gels in TBE (89 mM Tris-HCl, 89 mM boric acid, 2 mM EDTA). The bands were visualized by UV after staining with GelRed Nucleic Acid Stain (Biotium, Hayward, CA, USA).

Supplementary Figures

Figure S1. Stability of the GM-MITO-Porter in terms of diameter and ζ-potential

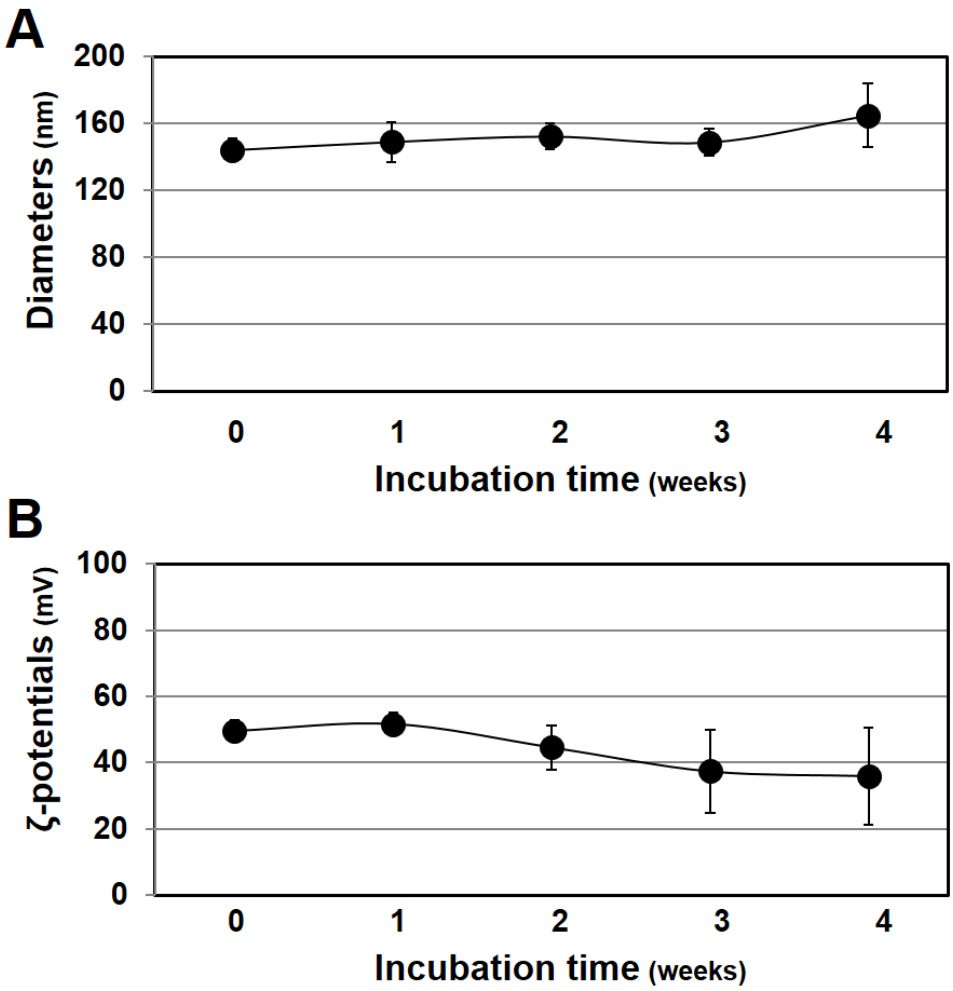

Fig. S1. GM-MITO-Porter was incubated in 10 mM HEPES buffer (pH=7.4) at 4°C, the diameters (**A**) and ζ−potentials (**B**) were measured at weekly intervals. Date are the mean ± S.D. (n=3).

Figure S2. Intracellular observation of naked NBD-GM in HeLa cells and PC12 cells.

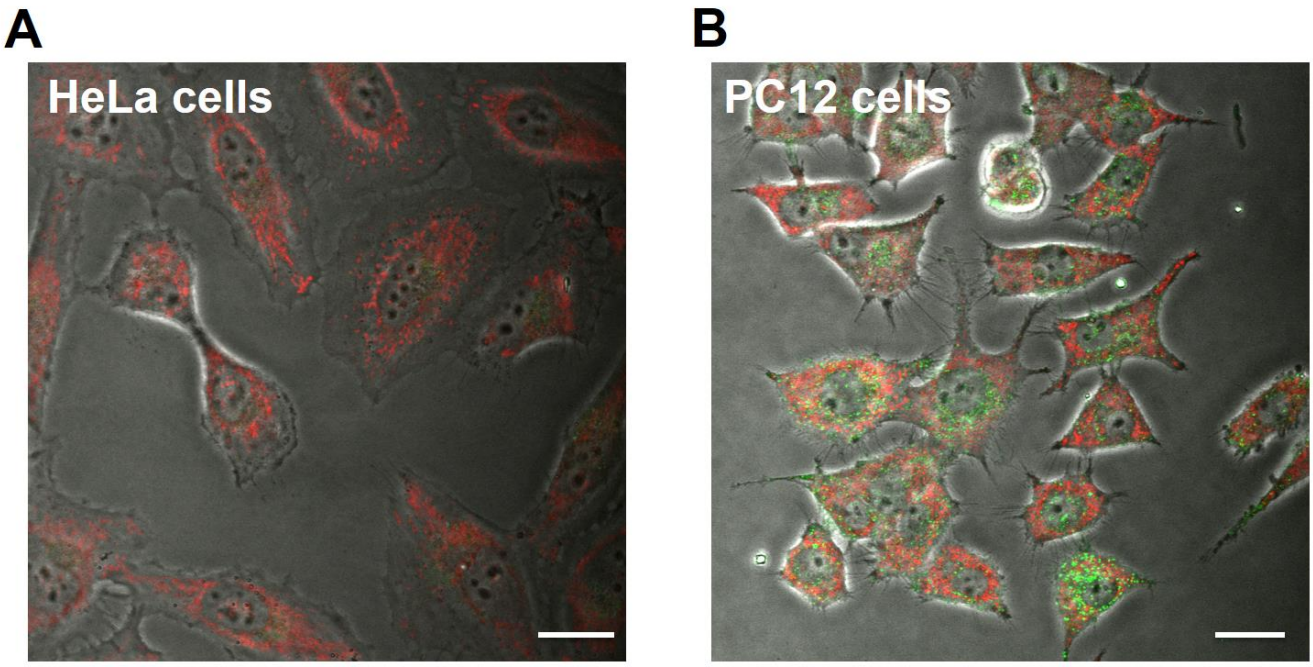

Fig. S2. Intracellular observation of NBD-GM (green color) in HeLa cells (**A**) and PC12 cells (**B**). The cells were treated with only naked NBD-GM at high applied dose (final concentration of NBD-GM, 1000 μM), and mitochondrial were stained with MitoTracker Deep Red FM (red color) prior to intracellular observation. Scale bars, 20μm.

Figure S3. Gel images of the RT–PCR detection of TRPV4-mRNA.

We performed RT-PCR assays to detect TRPV4-mRNA and GAPDH-mRNA (internal control) in the total RNA of HeLa cells (a human TRPV-4 negative cell), PC12 cells (a rat TRPV-4 positive cell) and HaCaT cells (a human TRPV-4 positive cell)[2]. Upper panel in Fig. S3 shows that the PCR product derived from rat TRPV-4 (403 bp) was present in PC12 cells (lane 4), while that from human TRPV-4 was not observed in HeLa cells (lane 2). We also confirmed that a band corresponding to human TRPV-4 (352 bp) was observed in HaCaT cell (a human TRPV-4 positive cell). In lower panel in Fig. 3, the PCR products derived from GAPDH-mRNA (internal control) were observed in all kinds of cells (lanes 2, 4, 6). These results suggest that the gene expression of TRPV4 was observed in the case of PC12 cells, but not in the case of HeLa cells. Moreover, gel images of RT–PCR detection showed that the target DNA bands disappeared in the absence of reverse transcription (RT(-)) (lanes 3, 5, 7), suggesting that contaminating DNA was not present when this RT–PCR assay was performed.

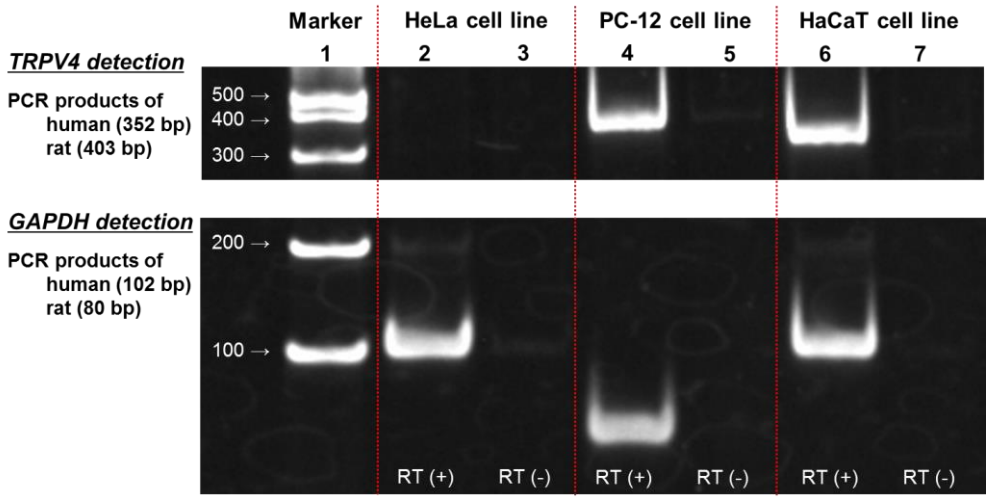

Fig. 3. Total RNA was purified from HeLa cells (lanes 2,3), PC-12 cells (lanes 4,5) or HaCaT cells (lanes 6,7) and PCR was done with specific primers for TRPV4 mRNA (upper panel) and GAPDH mRNA (lower panel) with reverse transcription (RT (+), lanes 2,4,6) and without reverse transcription (RT (-), lanes 3,5,7). In upper panel, the electrophoresis shows the PCR products derived from human TRPV-4 and rat TRPV-4 at 352 bp and 403 bp, respectively. In the lower panel, the electrophoresis shows the PCR products derived from human GAPDH and rat GAPDH at 102 bp and 80 bp, respectively. The PCR products were detected by the GelRed Nucleic Acid Stain after separation by electrophoresis. Lane 1, DNA Ladder.

Figure S4. Cell viability of empty MITO-Porter in HeLa cells.

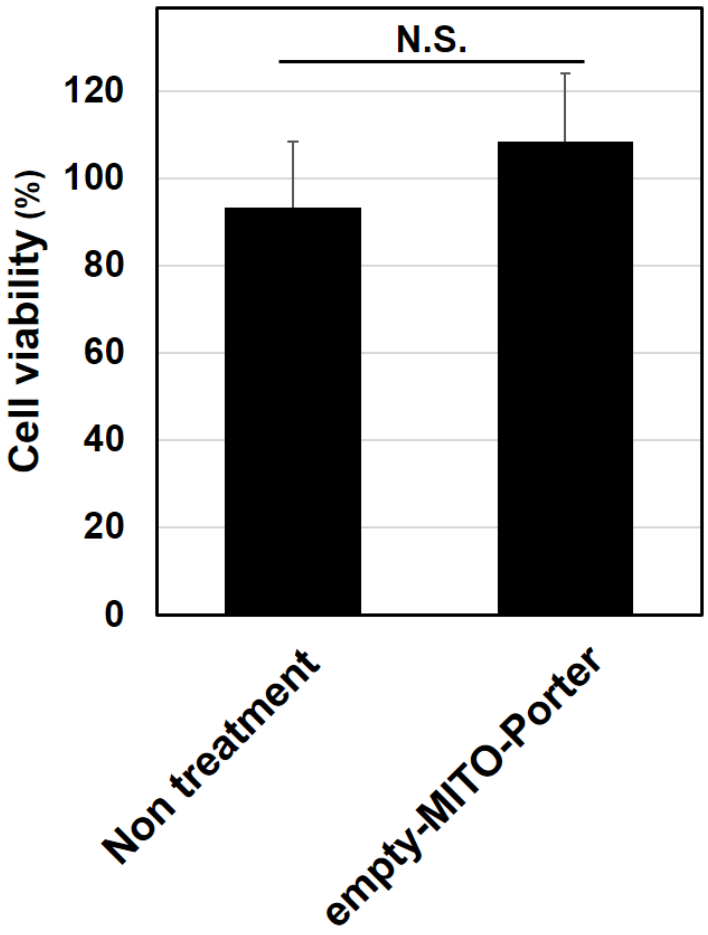

Fig. S4. Empty-MITO-Porters were added to HeLa cells (final concentration of the total lipid, 27.5 μM), and the cellular toxicity was evaluated at 48 hr after the incubation. Data are represented by the mean ± S.D. (n = 3). Significant differences were calculated by the student t-test and no significant difference (N.S.) were found. Note: lipid concentration of GM-MITO-Porter at 10 μM NBD-GM as shown in Figure 4A was about 10 μM.

References

1. Isoherranen N, Soback S 2000. Determination of gentamicins C(1), C(1a), and C(2) in plasma and urine by HPLC. Clin Chem 46(6 Pt 1):837-842.

2. Fusi C, Materazzi S, Minocci D, Maio V, Oranges T, Massi D, Nassini R 2014. Transient receptor potential vanilloid 4 (TRPV4) is downregulated in keratinocytes in human non-melanoma skin cancer. J Invest Dermatol 134(9):2408-2417.